Resveratrol improves health and survival of mice on a high-calorie diet

Joseph A. Baur*, Kevin J. Pearson*, Nathan L. Price, Hamish A. Jamieson, Carles Lerin, Avash Kalra, Vinayakumar V. Prabhu, Joanne S. Allard, Guillermo Lopez-Lluch, Kaitlyn Lewis, Paul J. Pistell, Suresh Poosala, Kevin G. Becker, Olivier Boss, Dana Gwinn, Mingyi Wang, Sharan Ramaswamy, Kenneth W. Fishbein, Richard G. Spencer, Edward G. Lakatta, David Le Couteur, Reuben J. Shaw, Placido Navas, Pere Puigserver, Donald K. Ingram, Rafael de Cabo, and David A. Sinclair

Supplementary Figures

Supplementary Figure 1

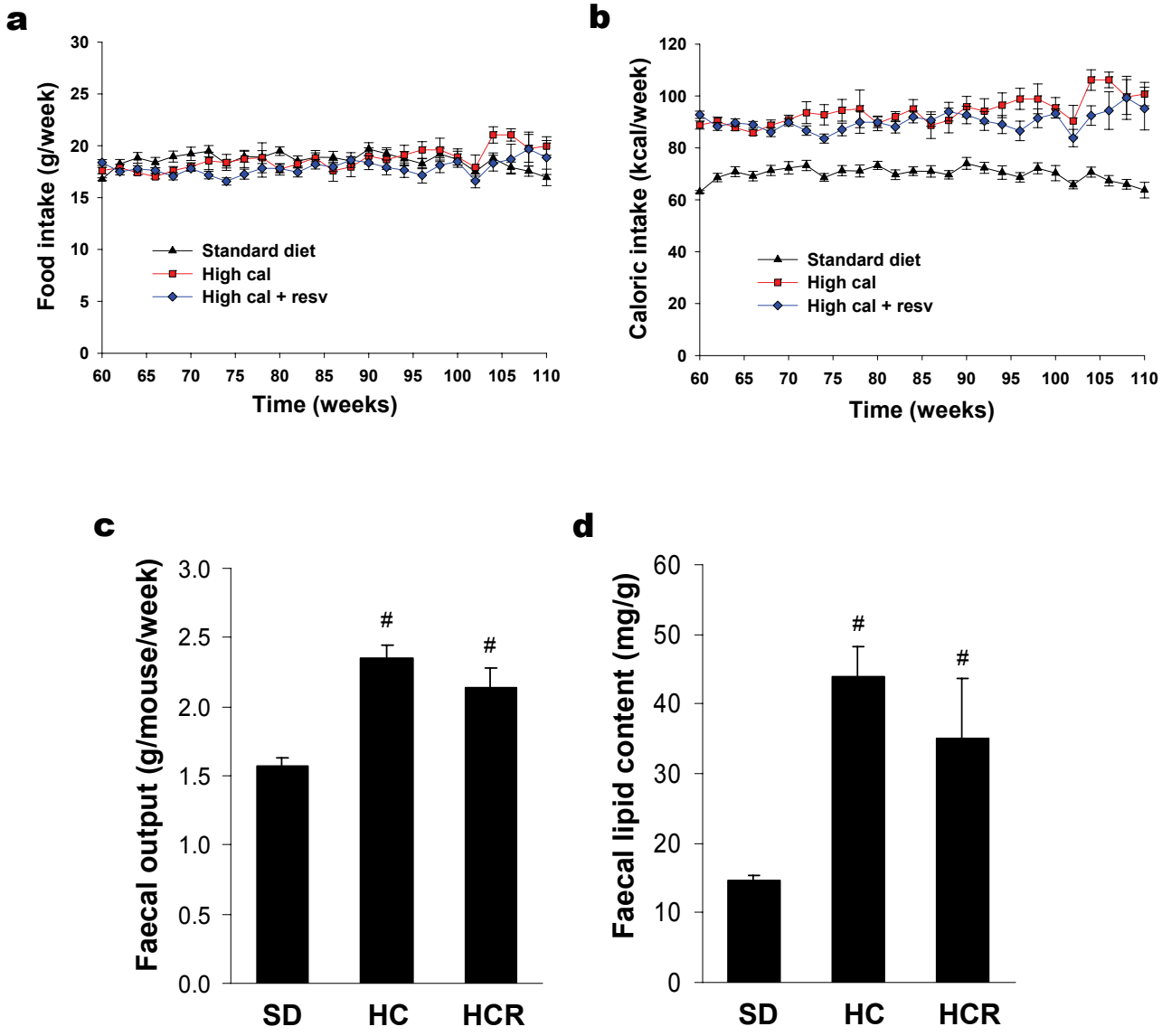

Supplementary Figure 1 | Total faecal output and faecal lipid content are not altered by resveratrol. a,b, Food intake by weight (a) or calories (b). **c,** Total faecal output; *n* = 3 cages (of 2-3 mice per cage). **d**, Lipid content of faeces. # - $p < 0.05$ vs. SD. Error bars indicate s.e.m.

Supplementary Figure 2

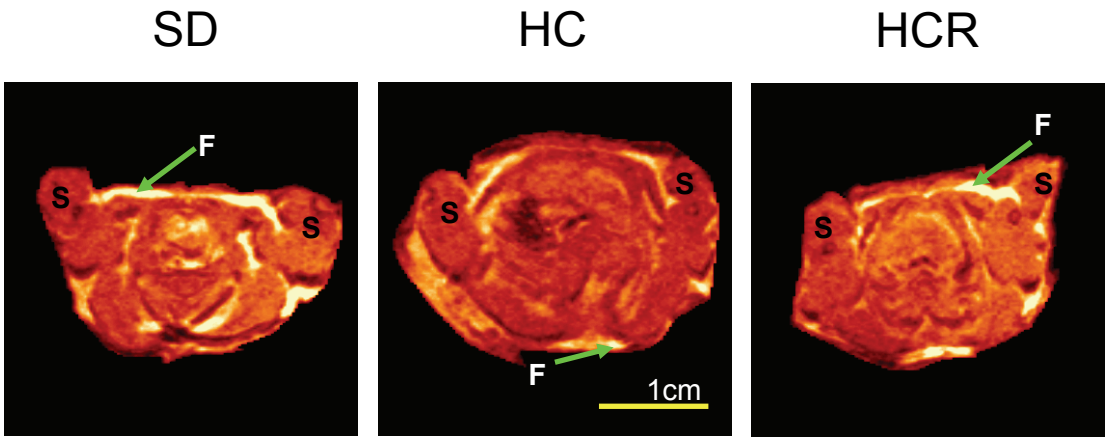

Supplementary Figure 2 | Fat distribution is not significantly changed by resveratrol as assessed by post-mortem MRI. T2-weighted proton spin-echo MR images acquired at 7 T showing fat distribution in 1 mm thick axial slices in mice from SD, HC, and HCR groups (n = 3 for each group) through the skeletal muscle of the shoulders (S). Images are presented with the anterior (ventral) side of each mouse facing the top of the image. Bright features at the periphery of the each mouse indicate subcutaneous or abdominal fat (F). No pronounced differences were observed in the post-mortem distribution of fat between subcutaneous, abdominal, and epididymal compartments or the distribution of brown fat between the three groups.

Supplementary Figure 3

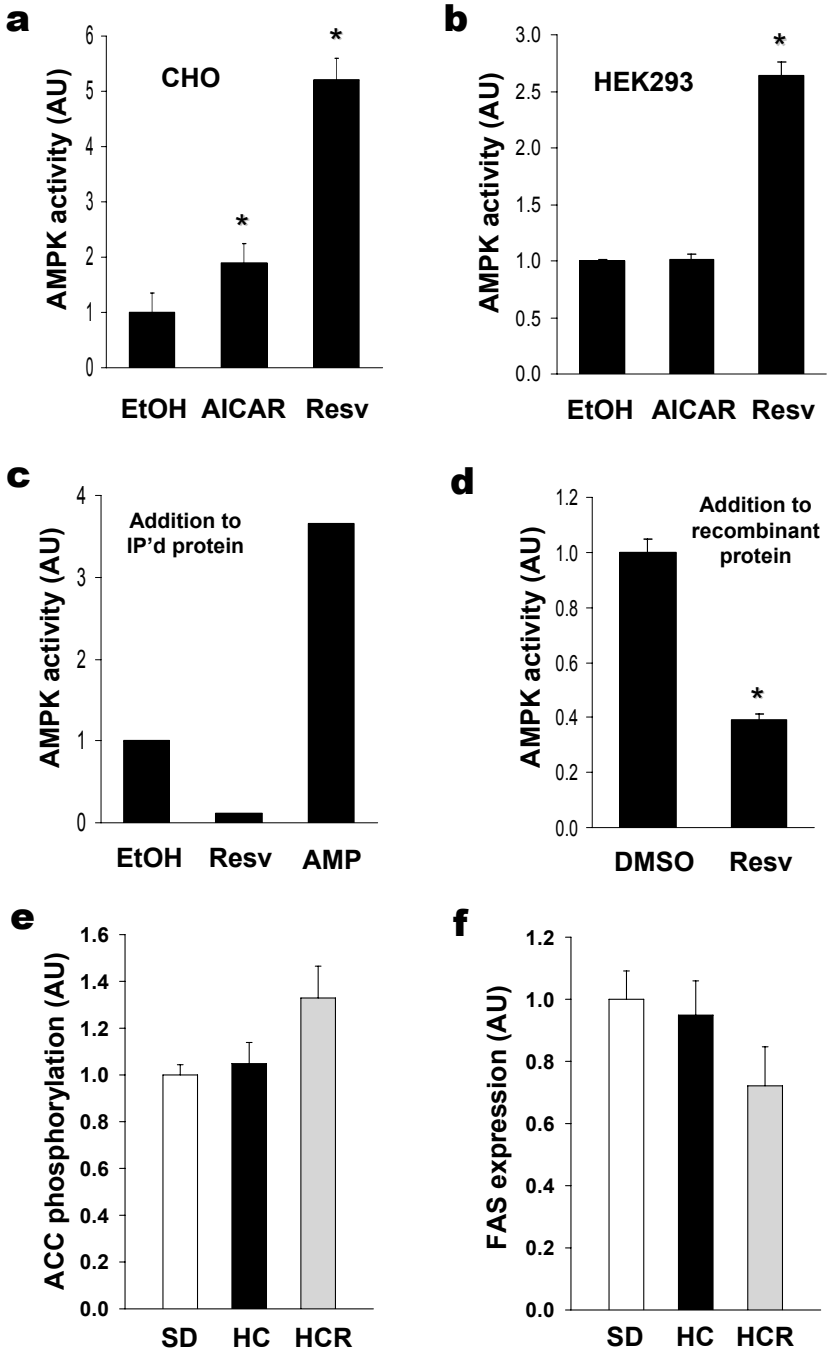

Supplementary Figure 3 | AMPK activity is enhanced via an indirect mechanism in cultured cells. a, b, The activity of Flag-tagged human AMPKα1 (co-transfected with HA-tagged human AMPKβ, and HA-tagged AMPKγ at a ratio of 2:1:1) following immunoprecipitation (IP) is enhanced by pre-treatment of CHO (a) or HEK293 (b) cells with 100 μM resveratrol. AICAR (2mM) is shown as a positive control, but was not effective in HEK293 cells. **c, d,** Adding resveratrol directly to the kinase reaction inhibits, rather than activates AMPK, consistent with its effects on several other kinases. Inhibition was observed with both immunoprecipitated (c) and purified recombinant (d) protein (100 and 20 μM resveratrol, respectively). **e,f,** Phosphorylation of ACC is increased (e), and expression of fatty acid synthase is decreased (f) in the livers of resveratrol-fed mice, both of which support the conclusion that AMPK activity is enhanced. *n* = 5 for all groups. * - $p < 0.05$. Error bars indicate s.e.m.

Supplementary Figure 4

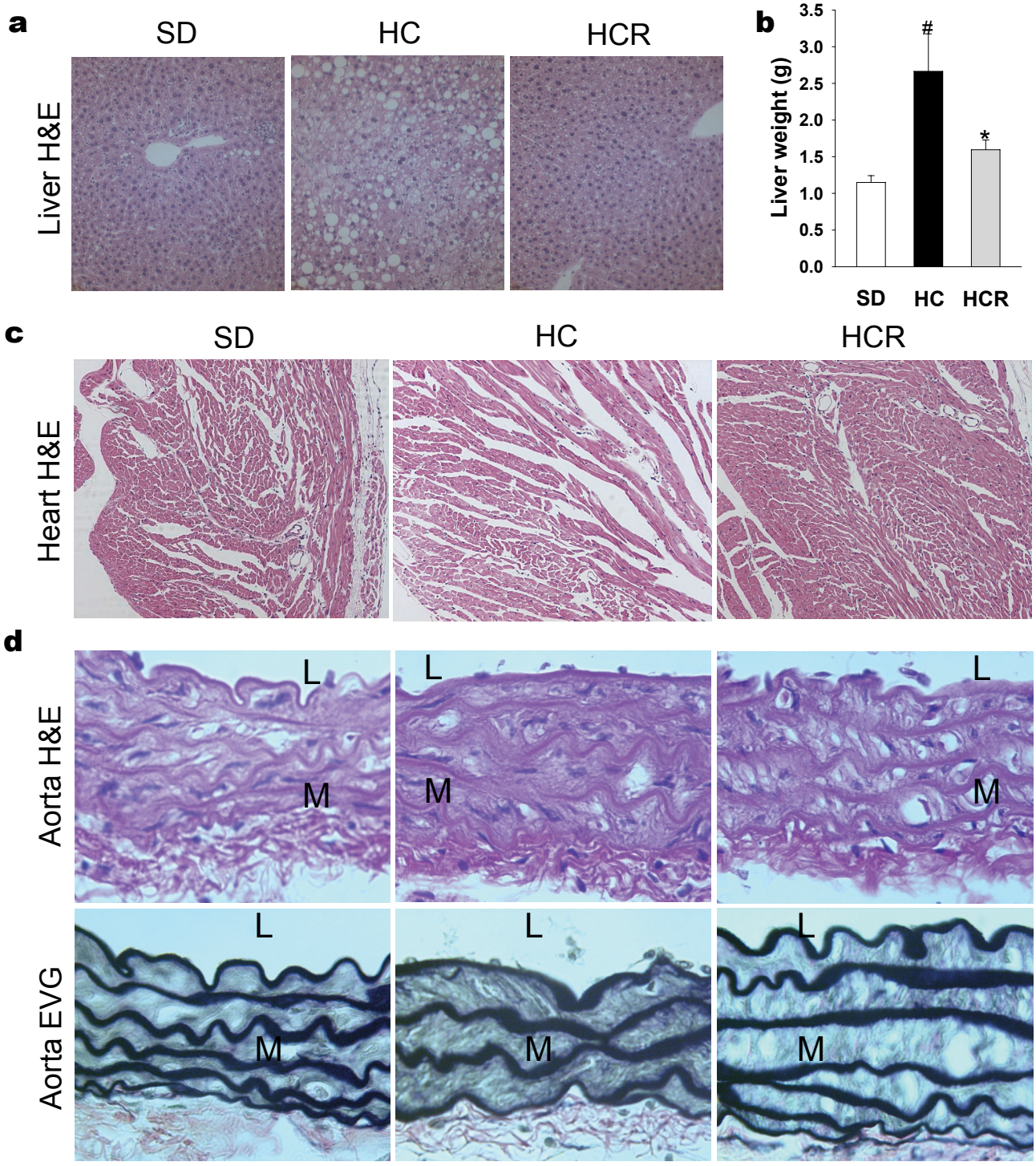

Supplementary Figure 4 | Resveratrol reduces pathological changes in the hearts of high calorie-fed mice. **a,** Representative hematoxylin and eosin (H&E) stained slices through the livers of animals from each group. **b,** Resveratrol prevents the increase in liver weight induced by the HC diet. **c,** The histology of HCR hearts is significantly improved, and is more similar to that of the SD group than HC controls, based on the white space and fatty infiltration between the individual cardiac fibers and fiber groups in the HC samples. The fibers in the HC group are also are thinner. In contrast, fibers are denser and less dispersed in the SD and HCR samples. Blinded pathology ratings are presented in Fig. 3d. **d,** Representative aortic sections stained with H&E (upper panels) or elastica van Gieson (EVG, lower panels). In HC mice, the aortic elastic lamina is straighter and less dense compared with SD samples. Interestingly, resveratrol preserves, at least in part, the wavy elastic fibers and retards the loss of aortic elastic density. *n* = 8 for panel b. M - media, L - lumen.

Supplementary Figure 5

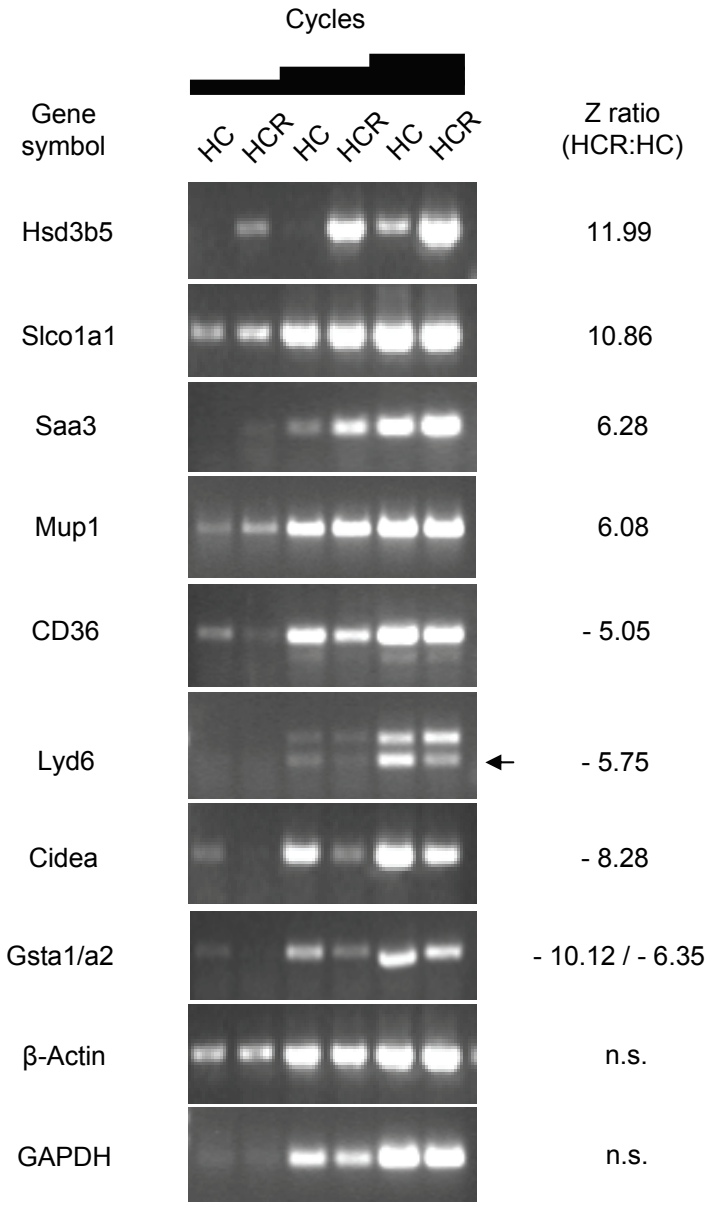

Supplementary Figure 5 | Validation of microarray results by RT-PCR. RNA from all animals in each group was pooled and amplified using primers specific for the indicated targets. For purposes of comparison, the Z scores obtained by microarray analysis are provided. Note that these numbers reflect statistical confidence and do not relate directly to fold-change. For Lyd6, the arrow indicates the size of the predicted product, while the upper band corresponds to the size predicted to result from amplification of genomic DNA (containing an additional 192 bp intron). A slight decrease in GAPDH mRNA in HCR relative to HC was consistently noted, while amplification of β-Actin mRNA was indistinguishable in all cases. n.s. - not significant.

Supplementary Figure 6

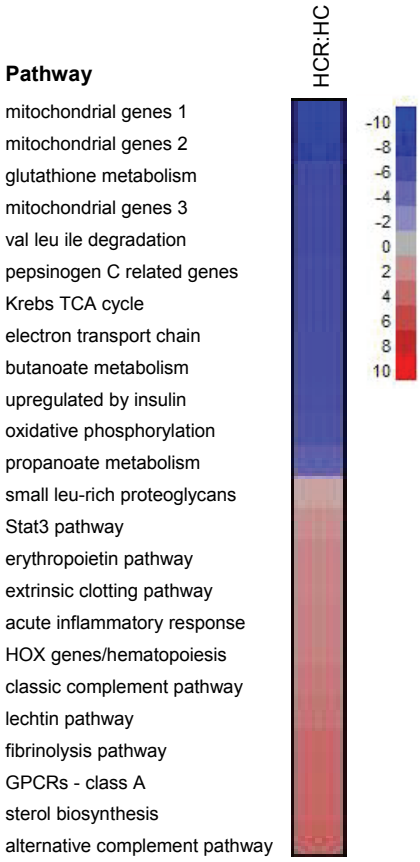

Supplementary Figure 6 | Comparison of the 12 pathways (gene sets) most highly up- (red) or down-regulated (blue) by resveratrol treatment. Some of the pathways have been given more descriptive names for the sake of clarity. Original names, as well as the complete list of significant changes can be found in figure S7a. The “acute inflammatory response” pathway appears to have been increased due to complement-related genes in the gene set and we did not observe evidence of a widespread inflammatory response.

Supplementary Figure 7a

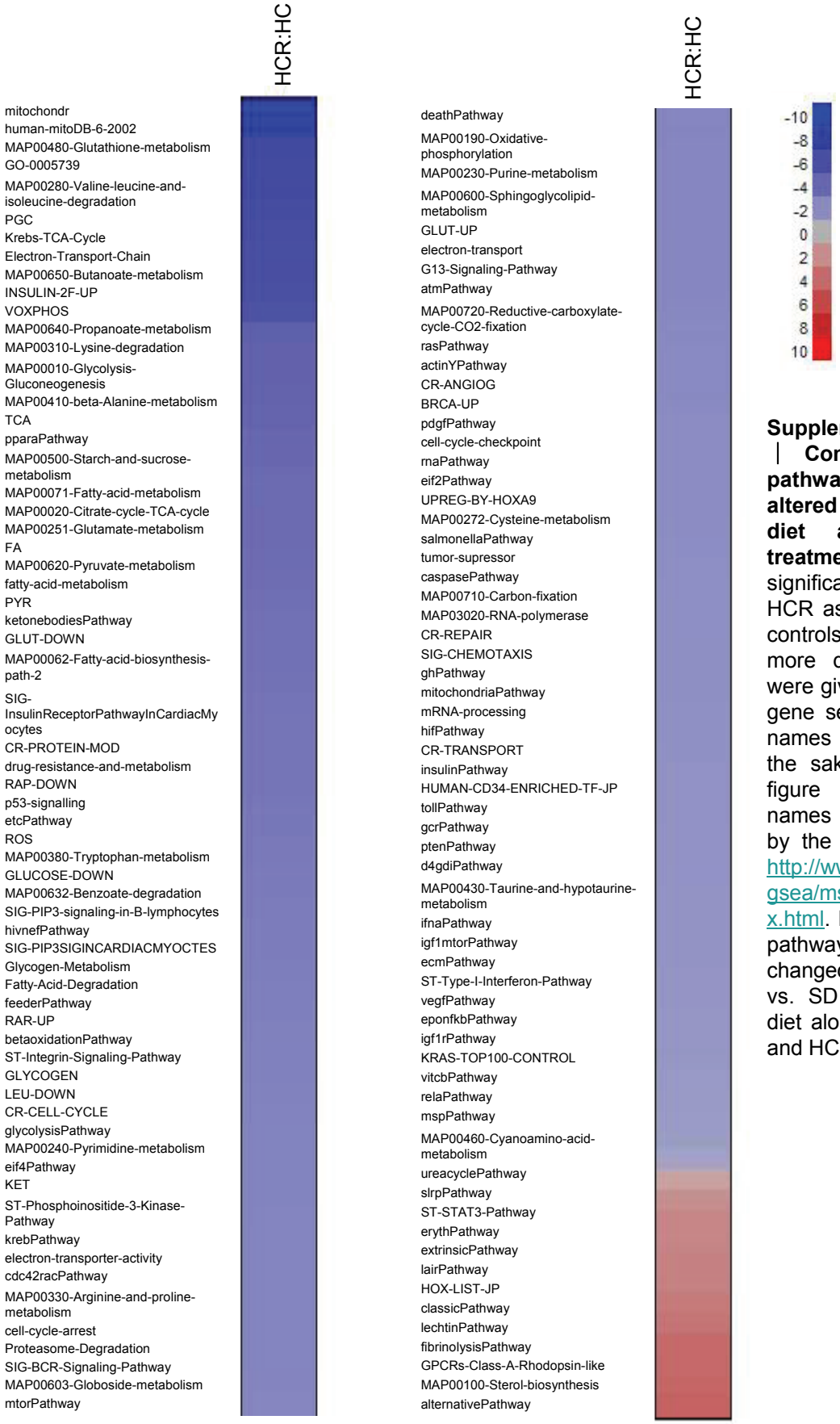

Supplementary Figure 7 | Complete listing of pathways significantly altered by high calorie diet and resveratrol treatment. a, Pathways significantly altered by the HCR as compared to HC controls. In Fig. 4 and S6, more descriptive names were given to some of the gene sets whose original names were esoteric, for the sake of clarity. This figure uses gene set names originally provided by the Broad Institute at http://www.broad.mit.edu/gsea/msigdb/msigdb_index.html. b, Complete list of pathways significantly changed by either HC diet vs. SD or HCR vs. HC diet alone. n = 5 for SD and HC, n = 4 for HCR.

Supplementary Figure 7b